

Retinal Ganglion Cell Types Contribute to Distinct Aspects of Visually Guided Prey Capture

Catherine Thériault

Department of Physiology
McGill University, Montreal

August 2022

A thesis submitted to McGill University in partial fulfillment of the requirements
for the degree of Master of Science.

© Catherine Thériault, 2022

Table of Contents

ABSTRACT	3
RÉSUMÉ.....	4
ACKNOWLEDGEMENTS.....	5
CONTRIBUTION OF AUTHORS.....	6
INTRODUCTION	7
Retinal Circuitry	7
Vertical organization	7
Lateral organization	8
Retinal Feature Detection and Circuitry	9
Direction Selective Retinal Ganglion Cells.....	9
Alpha Retinal Ganglion Cells	10
Central Projections.....	11
Image-forming	11
Non-image forming	12
Visually Guided Behaviours	12
Innate behaviours	13
Other behaviours	13
RATIONALE AND HYPOTHESIS.....	14

METHODS	14
Animals	14
Viruses	15
Stereotaxic Surgery	15
Cell Ablation and Silencing	15
Histology.....	16
Antibodies.....	16
DeepLabCut	16
Analysis.....	17
Behavioural Sequences.....	17
RESULTS	18
DISCUSSION.....	28
CONCLUSION.....	31
REFERENCES	32

Abstract

The visual scene is encoded by circuits of the retina as several parallel representations, each containing emphasis on a specific aspect of the scene such as motion or edges. These representations make it to the brain via output neurons, called retinal ganglion cells (RGCs), which are unique to each retinal circuit and grow axons via the optic nerve into the brain for further analysis. How do these representations support visually guided behaviour? Do individual RGC signals directly inform aspects of a visual behaviour? Or does the brain recombine RGC signals to drive behaviour? To address these issues, I trained mice to perform a visually guided prey capture assay and studied their performance in the presence and absence of specific RGC types. First, I recorded videos of prey capture and segmented behaviour into 7 syllables called approach, pursuit, contact, exploration, flight, freeze, and capture. By examining the spatio-temporal structure of these syllables across hunting trials and by examining how mice transit from one syllable to another I show that hunting comprises a highly stereotyped sequence of actions. Next, I employed chemogenetic silencing and ablation tools to remove RGCs that sense directional motion(DSGC) or those more sensitive to contrast/form(α RGC) and studied the consequences on hunting syllables. I observed that a generalized loss of pursuit-contact and approach-pursuit transitions. However, mice lacking α RGCs spent far more time in explore-freeze states than did mice with disrupted DSGCs. Taken together these data show that RGCs contribute to distinct aspects of visually guided prey capture.

Résumé

La scène visuelle est codée par les circuits de la rétine en plusieurs représentations parallèles, chacune soulignant un aspect spécifique de la scène, tel que le mouvement ou le contraste. Ces représentations parviennent au cerveau par des cellules ganglionnaires de la rétine (RGC), qui sont uniques à chaque circuit rétinien et font pousser des axones jusqu'au cerveau via le nerf optique pour une analyse plus approfondie. Comment ces représentations soutiennent-elles les comportements guidés par la vue ? Les signaux individuels des cellules rétiniennes informent-ils directement les aspects d'un comportement visuel ? Ou bien le cerveau recombine-t-il les signaux des RGC pour guider ces comportements ? Pour répondre à ces questions, j'ai entraîné des souris à effectuer un test de capture de proie guidée visuellement et j'ai étudié leurs performances en présence et en l'absence de types spécifiques de RGC. Tout d'abord, j'ai enregistré des vidéos du test de capture de proie et j'ai segmenté le comportement en 7 syllabes principales appelées approche, poursuite, contact, vol, gel, exploration et capture. En examinant la structure spatio-temporelle de ces syllabes pendant les chasses et en examinant comment les souris passent d'un comportement à un autre, je démontre que la chasse est composée d'une séquence d'actions hautement stéréotypées. Ensuite, j'ai utilisé des outils de silençage et d'ablation chimio génétiques pour éliminer les RGC qui détectent les mouvements directionnels (DSGC) ou ceux qui sont plus sensibles au contraste/à la forme (α RGC) et j'ai étudié les conséquences sur les syllabes de chasse. J'ai observé une perte généralisée des transitions poursuite-contact et approche-poursuite. Cependant, les souris dépourvues de α RGC passaient beaucoup plus de temps dans des états d'exploration-arrêt que les souris dont les DSGC étaient perturbés. L'ensemble de ces données montre que les RGCs contribuent à des aspects distincts de la capture de proies guidée visuellement.

Acknowledgements

I couldn't have done this degree without the help and support of those around me. I would like to first and foremost thank my supervisor Dr. Arjun Krishnaswamy for taking a chance on me when he first hired me. His incredible support and guidance have pushed me to be a better, more confident scientist. Next, I would like to thank my lab mates Pierre-Luc, Aline, Jonas and Ku for being some of the best people to work and have lunch with. You guys made this whole experience (and covid!) so much better, and I sincerely appreciate your support through it all. I would also like to thank my family and friends for their encouragement throughout my degree, and for cheering me up when things got difficult. Finally, I would like to thank Drs. Reza Sharif-Naeini, Aparna Suvrathan, Michael Hendricks for serving on my committee and Dr. Erik Cook for his help and advice.

Contribution of Authors

The author contributed to the development of the various surgical procedures and behavioural assays, performed immunohistology and imaging of samples. The author performed data analysis, with assistance from Dr. Arjun Krishnaswamy and Dr. Kuwook Cha. The author wrote this thesis, with guidance and revision of Dr. Arjun Krishnaswamy.

Introduction

Vision starts after light enters the lens of the eye and strikes a thin sheet of neural tissue, which lines the back surface of the sclera, called the retina. Current models suggest that the mouse retina encodes the visual scene as a series of parallel representations, each contains emphasis on a particular visual feature such as motion. Each representation is carried to the brain along a particular retinal ganglion cell's (RGC) axon which innervates specific brain regions. Approximately 40 different brain regions receive input from the retina, and in many cases receive input from specific RGC types. These observations raise questions about the behavioral significance of a given RGC type's visual signals. Below, I outline the principal cell types of the retina with particular focus on RGCs and their feature computations.

Retinal Circuitry

Vertical organization

Vision begins when light strikes the photoreceptors (PR). There are two distinct classes of PRs in the vertebrates: cones which compose 3% of the mouse retina and rods which accounts for 97% of the retina (Carter-Dawson & Lavail, 1979; Lolley & Lee, 1990; Nikonov et al., 2006). Rods can detect and signal the absorption of a single photon, which makes them very light sensitive and best suited for low light (scotopic) vision. Cones are less sensitive and are used for bright light (photopic) vision but show quicker adaptation to light changes (Rodieck, 1998) and come in three types, each expressing one of three opsins (short, medium, and long wavelength), which allow for the basis for hue differentiation, and therefore colours vision (Nikonov et al., 2006).

Photoreceptors signal to Bipolar cells (BC). There are several types of BCs, however the dendritic processes of BCs only receive input from either cones or rods, rarely both (Wassle et al., 2009). BCs are named for their oppositely oriented axons and dendrites which link the outer and inner retina. BC dendrites collect input from PRs in the outer plexiform layer then project stratified axons into the inner plexiform layer (Euler &

Masland, 2000; Shen et al., 2009). BCs separate in the PR input into different properties such as light-onset, light-offset, contrast, colour and speed(Euler et al., 2014).

There are two inhibitory circuits in the visual pathway, the first involving horizontal cells (HC), and the second involving amacrine cells (AC). HCs help modulate glutamate release from the PRs, which is theorized to help PR adapt to different illumination levels in the environment(Twig et al., 2003) . HCs are also involved in the pathways that regulate color opponency and contrast (Masland, 2001). The second inhibitory pathway is mediated by ACs in the inner plexiform layer where they modulate visual signals (Jeon et al., 1998). Briefly, ACs receives input from BC and other ACs while also providing input to AC and RGCs. With a few exceptions, ACs are inhibitory neurons that release either GABA or Glycine and are the most diverse retinal type with around 50 different subtypes(Macosko et al., 2015). This cellular diversity is paralleled by their functional diversity which include important roles in object motion detection, motion direction sensing, looming detection, etc (Demb, 2007; Grimes et al., 2010; Huberman et al., 2008; MacNeil & Masland, 1998).

RGCs are the last step in the retinal visual pathway and integrate visual input from a specific subset of ACs and BCs to become attuned to a particular feature of the visual scene. Each RGC type then sends this feature report to the brain via the optic nerve (Martersteck et al., 2017; Seabrook et al., 2017; Shi et al., 2019; Varadarajan & Huberman, 2018). These features include motion-detection, direction selectivity, orientation selectivity, colour, contrast etc. (Gollisch & Meister, 2010; Sanes & Masland, 2015; Seabrook et al., 2017), and it has been shown that there are over 40 different types of RGCs (Baden et al., 2016; Rheume et al., 2018; Sanes & Masland, 2015; Tran et al., 2019). This diversity of signals paired with the diversity of retinal targets raises questions about the behavioral significance of these RGC features.

Lateral organization

It has previously been shown that each individual RGC type is evenly spaced out across the retina, which permits each cell type to detect its preferred feature from the entire visual scene (Reese & Galli-Resta, 2002; Sanes & Masland, 2015). The minimal spacing

around neighbouring cells is called the “exclusion zone” and is an intrinsic property of each RGC type (Bleckert et al., 2014; Masland, 2001). These patterns are called ‘mosaics’ (Sanes & Masland, 2015), and the distribution of these neurons can be arranged in such a way to enhance specific features or regions of a visual scene (Bleckert et al., 2014). For example, PR and RGC density increases to form a fovea-like area in the mouse retina with enhanced visual acuity (van Beest et al., 2021) and mouse α RGCs display differences in cell density and size across the retina in a nasal to temporal patterns. This α RGC pattern permits for increased acuity in the frontal visual fields, which suggests that different rgc types may have differently organized topography to encode specific features (Bleckert et al., 2014)

Retinal Feature Detection and Circuitry

We currently know there are around 40 different RGC types, accounting for over 95% of all RGCs in the retina with 5% still unknown (Martersteck et al., 2017; Sanes & Masland, 2015). Most RGC types are not functionally well characterized (Goetz et al., 2022). However extensive research has been conducted on the densest cell types like w3b, mini-j-rgc, jam-b, ON-OFF DSGCs etc. Below, I describe the basic circuitry and feature computations of two kinds of RGC that I used in my experiments.

Direction Selective Retinal Ganglion Cells

The mouse retina dedicates around 20% of its output to compute motion direction (Wei, 2018). There are two main categories of RGCs involved, the ON direction selective (DS) RGC (OnDSGC) which responds to light increment, and the ON-OFF DSGC (ooDSGC) which also respond to light decrements. There are four types of ON-Off DSGC, each preferring motion in one of the cardinal directions: nasal, temporal, superior and inferior (Reinhard et al., 2019; Wei, 2018).

Starburst amacrine cells (SACs) play an important role in direction selectivity. ON SACs inhibit ON DSGCs, while ON and OFF SACs inhibit ooDSGC (Euler et al., 2002). When SACs are silenced or killed, DSGCs no longer have a preferred motion, firing to all directions (Pei et al., 2015; M. Yoshida & Hasselmo, 2009). The dendrites of the SAC independently sense motion and release GABA onto ooDSGCs which results in the

preferred motion direction of each ooDSGC to oppose that of the SAC dendrites innervating them (Euler et al., 2002; Poleg-Polsky et al., 2018). ooDSGCs have bistratified dendrites, which are also innervated by ON and OFF BCs, which recent studies have shown might be DS (Matsumoto et al., 2019). As for ON DSGCs, they receive input from 4 ON BC types (Matsumoto et al., 2019) whose glutamatergic inputs are arranged asymmetrically across the RGC dendrites. This causes preferred motion to activate slower inputs before faster ones, allowing for a larger summed response and contributing to ON DSGC preferences to slow moving stimuli (Dhande et al., 2013; Gauvain & Murphy, 2015; Matsumoto et al., 2019) There are 3 different ON DSGCs with different direction preference (superior, inferior and temporal), morphologies and marker expression (Dhande et al., 2013; Martersteck et al., 2017; Yonehara et al., 2009).

After leaving the retina, ooDSGCs primarily innervate the SC and the shell of the dLGN; neurons in this latter structure then innervate primary visual cortex (V1) layers 2 and 3 (Cruz-Martín et al., 2014; Matsumoto et al., 2019; Reinhard et al., 2019; Seabrook et al., 2017). SC integrates visual, auditory, and somatosensory information to direct orienting behaviours such as attention, and relevant to this thesis, prey capture (Cang et al., 2018; Hoy et al., 2016; Ito & Feldheim, 2018). The top of the superficial SC is innervated by ooDSGCs, and many neurons in this area are also DS (de Malmazet et al., 2018; Ito et al., 2017; Shi et al., 2019). As for the ON DSGC, axons primarily innervate the accessory optic system (AOS) which is made up of the medial terminal nucleus (MTN), the dorsal terminal nucleus (DTN) and the nucleus of the optic tract (NOT) (Simpson, n.d). These regions are involved in two gaze-stabilizing reflexes that are potentially used during prey capture: the optokinetic reflex and the vestibulo-ocular reflex (Matsumoto et al., 2019; K. Yoshida et al., 2001). While ON DSGCs innervate all three areas, ooDSGCs only innervate the NOT and DTN (Dhande et al., 2013; Kay et al., 2011; Yonehara et al., 2009).

Alpha Retinal Ganglion Cells

There are three types of well studied α RGCs: sustained ON response (sON α), sustained OFF response (sOFF α) and transient OFF response (tOFF α)(Dunn et al., 2006;

Margolis & Detwiler, 2007; Pang et al., 2003). sON α and sOFF α are paramorphic pairs, but they differ in their circuits (Boycott & Wässle, 1974; Soto et al., 2020). The sON α receptive fields are nonlinear, which permits this cell type to respond to patterns such as gratings (Dunn et al., 2006; Pang et al., 2003) and sON α receive excitatory input from ON BC and inhibitory input from ACs that are driven by these BCs. sOFF α and tOff α RGCs are excited by OFF BCs, while sOFF α RGCs are also excited by VGLUT₃ ACs and inhibited by All ACs (Dunn et al., 2006; Kim et al., 2020; Krishnaswamy et al., 2015; Pang et al., 2003). This circuit is crucial for looming triggered defensive responses, as it encodes the size of an overhead object (Krieger et al., 2017; Wang et al., 2021; Yilmaz & Meister, 2013). Recent studies have shown that there is a 4th lesser known type, paramorphic to tOff α , called the tON α (Krieger et al., 2017). This cell type also integrates spatial information nonlinearly and expresses the same markers as other α RGCs (e.g. SMI₃₂ and SPP₁). The underlying circuits of this type are not well characterized (Krieger et al., 2017; Tran et al., 2019).

Central Projections

The central projections of mouse RGCs are diverse but can be grouped into image-forming and non-image forming pathways.

Image-forming

RGC feature signals are sent to over 40 distinct areas in the brain where they are further processed and used to drive behaviours (Martersteck et al., 2017). These inputs synapse on the dLGN in the thalamus, where the information is then passed to the visual cortex. SC is another important retinorecipient area which permits animals to identify environmental features and modify innate behaviours (Krauzlis et al., 2013). Two RGC types of interest are the α RGC, which projects to the core of the dLGN as well as in the deeper layers on SC, and the ooDSGCs that project to the shell of the dLGN and superficial layers on SC (Martersteck et al., 2017). Thalamocortical relay neurons in the shell region of the dLGN sends their axons to layers 1 and 2/3 of V₁ while the neurons in the core region send their axons to layers 4 and 5/6 (Seabrook et al., 2017).

Non-image forming

While RGCs project to >40 different brain regions, not all these regions are image-forming. Non-image forming circuits help support image forming circuits indirectly through sub-conscious reflexive behaviours such as pupil, image stabilization, and circadian reflexes (Dhande et al., 2013; Hatori et al., 2008; Seabrook et al., 2017). These phenomena rely on visual cues but have no relationship to sight. A type of RGC, the M1 ipRGC is non image forming, but the ablation of these cells disrupts the circadian rhythm (Hatori et al., 2008) as well as pupillary responses (J. W. Chen et al., 2011). Almost all non-image forming retinorecipient areas receive input from the cortex (Liu et al., 2016). However, except for recently discovered retinorecipient areas, such as the amygdala, non-image forming areas do not project into cortex.

Visually Guided Behaviours

The growing ability we genetic access to individual RGC types is opening important avenues to ask what purpose their signals serve in visual behaviour.

Direction selective RGCs are involved in two gaze-stabilizing reflexes, the optokinetic reflex and the vestibulo-ocular reflex (Yonehara et al., 2009; K. Yoshida et al., 2001). Due to this, deficits in DS neurons in layer 2 of V1 disrupts optic flow when moving forward, making it difficult for mice to stabilize their visual field (Rasmussen et al., 2021). For visually-guided hunting behaviour, zebrafish lacking these RGCs have been shown to lack orienting behaviour affecting capture rates (Gahtan, 2005). Disruptions of DS neurons of the SC can also impair detection and pursuit of prey, while the ablation wide-field motion sensitive SC neurons also impairs detection of prey (Hoy et al., 2019; Morrie & Feller, 2017). Another type of visually guided behaviour is looming behaviour, where mice escape an enlarging circle above head. W3 and tOFF α RGCs are known to regulate looming behaviour, and research has shown ablating RGCs impair escape and freezing behaviours (Wang et al., 2021).

Innate behaviours

There are certain innate behaviours that mice will display for survival such as avoiding predators or looking for food (Hoy et al., 2016; Yilmaz & Meister, 2013). Studies have demonstrated that showing a mouse a black circle expanding overhead will trigger a freeze or escape response while a white circle triggers no behaviours (Kerschensteiner, 2022; Kim et al., 2020; Wang et al., 2021; Yilmaz & Meister, 2013). This demonstrates that it takes certain features, such as expanding dark objects to trigger specific behaviours. The SC has been linked with this phenomenon, as the neurons on the superficial layer show activity during looming behaviour (Wei, 2018).

Mice in the wild are prolific hunters as they catch small insects, sometimes relying on this skill for survival (Langley, 1989). The standard lab mouse can also develop this ability within a few days, a behaviour called innate prey-capture (Hoy et al., 2016). This behaviour relies solely on vision, as the mouse orients itself towards the cricket to begin the hunt. The mouse continuously readjusts its position while stalking its prey, until capture occurs (Hoy et al., 2016). The aforementioned vestibulo ocular reflex is likely to be crucial for hunting since a recent study shows that mice stabilized the image of their prey in a small area of the temporal retina (Holmgren et al., 2021). Furthermore, Johnson et al (2021) demonstrated that mice kept prey within their binocular field, suggesting that ipsilaterally projecting ganglion cells are used to guide prey capture. 5 of 9 ipsilaterally projecting RGCs are involved, and the ablation of these results in impaired hunting success (K. P. Johnson et al., 2021).

Other behaviours

Through the course of my MSc, I developed an assay to measure visual contributions to social behaviours. Social behaviours usually integrate multiple sensory modalities, both individually but more often in a combination of olfactory, visual and auditory cues (P. Chen & Hong, 2018). Mice are able to recognize one another and discriminate between littermate or stranger mouse (Moy et al., 2004). It is known that olfactory and auditory cues are crucial to social communication in mice however little is known about the role of vision in social behaviour (Crawley, 2007). To explore this potential role, I built a modified version of a 3-

chamber box (Moy et al., 2004) where the stranger mouse was held in clear container with no holes to try to isolate visual behaviour. The idea was to examine how much time a mouse spends with each stranger mouse in the presence and absence of specific RGC types (ie: α RGCs). I completed baseline studies to validate this apparatus and developed analysis code. These studies, together with my results on RGC contributions to innate visual prey capture will allow future experiments to study RGC contributions to social behaviour.

Rationale and Hypothesis

Rationale: Each RGC type senses a unique feature in the visual scene but the role of these features in visual behaviour is not well explored. To learn more, I will train mice in an innate prey-capture behaviour and study their performance after selectively ablating/silencing α RGC and DSGCs.

Hypothesis: I hypothesize that ablation/silencing of DSGCs and α RGC RGCs will affect different aspects of hunting behaviour.

Methods

Animals

Animals were used in accordance with the rules and regulations established by the Canadian Council on Animal Care and protocols were approved by the Animal Care Committee at McGill University. Male and female ChAT-IRES-Cre, KCNG4-Cre and Vglut2-Cre mice aged 35–100 days old were used in this study. Vglut2-Cre mice were obtained from the Jackson Laboratory (*Slc17a6*-Cre, Jackson Labs, RRID:[IMSR_JAX: 016963](#)). KCNG4-Cre mice were obtained from the Jackson Laboratory (B6.129(SJL)-Kcng4tm1.1(cre)Jrs/J, Jackson Labs, RRID: [IMSR_JAX: 029414](#)). ChAT-Cre mice were obtained from the Jackson Laboratory (B6;129S6-Chattm2(cre)Lowl/J, Jackson Labs, RRID: [IMSR_JAX: 006410](#)).

Viruses

AAV retro hSyn-DIO-hM₄D(Gi)-mCherry is a Cre-dependent and hSyn-driven hM₄D(Gi) receptor with an mCherry reporter for CNO-induced neuronal inhibition. (Addgene viral prep # 44362-AAV9, <http://nzt.net/addgene:44362>, RRID: Addgene_44362) aav2/retro-CAG-flex-DTR is a cre-dependent diphtheria toxin receptor, which then requires diphtheria toxin for targeted cell ablation (Canadian Neurophotonics Platform Viral Vector Core Facility, RRID:SCR_016477).

Stereotaxic Surgery

AAVs were injected primarily intraocularly to label ChAT-cre, KCNG₄-Cre or Vglut2-Cre RGCs, though some injections were preformed intracranially. For the intraocular injection, mice were anesthetized using isoflurane (2.5% in O₂) and given subcutaneous carprofen as analgesic. A small 1mm incision posterior was made on the eye posterior to the ora serrata and the virus was injected using a bevelled Hamilton syringe (7803-05, 7634-01, Hamilton). Mice were given a week to recover.

For intracranial injections, the mice were anesthetized as above and for analgesia given subcutaneous carprofen and a mixture of local bupivacaine/lidocaine mix. Once transferred to a stereotaxic apparatus, a small craniotomy (>1 mm) was made in the appropriate location of the skull using a dental drill. A Neuros syringe (65460-03, Hamilton) filled with virus was then lowered into the LGN (2.15 mm posterior from bregma, 2.27 mm lateral from the midline and 2.75 mm below the pia) using a stereotaxic manipulator. A micro syringe pump (UMP3-4, World Precision Instrument, Sarasota, FL) was used to infuse 400 nL of virus (15 nL/s) bilaterally in dLGN the bolus allowed to equilibrate for 8 min before removing the needle. Mice were given 2 weeks to recover

Cell Ablation and Silencing

Powdered Clozapine N-oxide (CNO, Abcam; RRID: ab141704) was dissolved in dimethyl sulfoxide to 1mg/mL. CNO was then injected intraperitoneally at a dosage of 1

mg/kg. Peak CNO activation occurs 30 minutes post injection (Manvich et al., 2018). Mice were injected 25 minutes pre-trial.

Diphtheria Toxin was dissolved in PBS to 1 mg/mL. DT was then injected intraperitoneally at a dose of 1 20ug/kg. Peak DTR inactivation occurs 12-24 hours after injection and is permanent (V. G. Johnson et al., 1988). Mice were injected 18 hours pre-trial.

Histology

Following isoflurane overdose euthanasia, mice were transcardially perfused first by chilled PBS, then by 4%(w/v) paraformaldehyde (PFA) in PBS and enucleated. Eyes were fixed for an additional 45 minutes in 4%(w/v) PFA. Dissected retinal tissue was then incubated in a 4% blocking buffer (4% donkey serum/0.4% Triton X-100/PBS) with primary antibody for 7 days at 4C and incubated in secondary antibodies overnight at 4C. After a few washes in PBS, the tissue was flat-mounted on membrane filters and cover slipped with Fluoromont Aqueous Mounting Medium (Sigma-Aldrich).

Antibodies

Antibodies used: mouse anti-Ap2- α (1:100, clone 3b5 from Developmental Studies Hybridoma Bank, Iowa City, IA); rabbit anti-DsRed (1:1000, Clontech Laboratories; RRID:AB_10013483); goat Anti-Choline Acetyltransferase (1:1000, MilliporeSigma; RRID:AB144P); goat anti-osteopontin (1:1000, R&D Systems; RRID:AB_2194992); guinea pig anti-RBPMS (1:100, Phosphosolutions; RRID:AB_2492226). Secondary antibodies were conjugated to Alexa Fluor 405 (Abcam; RRID: AB_2715515), Alexa Fluor 488 (Cedarlane, Ontario, CA; RRID:AB_2340375), Cy3 (MilliporeSigma; RRID:AB_92588, RRID:AB_92570, or Jackson ImmunoResearch, West Grove, PA; RRID:AB_2340460) or Alexa Fluor 647 (MilliporeSigma; RRID:AB_2687879).

DeepLabCut

DeepLabCut (DLC, Mathis et al., 2018) is a markerless estimation pose software which I used to track mouse and cricket position. To train the network, I chose 4 points on

the mouse (right and left ear, nose, tail base) and one point on the cricket. DLC used these points to train a network, which allowed for analysis of all prey capture videos. DLC output includes body part coordinates for all videos frames, which was then analyzed using a custom MATLAB script.

Analysis

DLC generated body part coordinates were used to track both mouse and cricket position, which was filtered to remove non-representative data (DLC likelihood < 0.97). To determine mouse head position, a head mid-point coordinate was calculated using both right and left ears coordinates. The nose coordinates were then used to calculate mouse head direction which references to the vector between the nose and center of the mouse head. I used this to define azimuth, which is the angle of the cricket relative to the mouse, as well as distance to the cricket (range). Mouse and cricket velocity was also measured, by calculating the difference in head coordinates for each frame. These variables were then used to define different syllables of prey capture behaviour.

Behavioural Sequences

6 different sub-behaviours, defined as syllables, were extracted from our analysis. First, I defined a contact as range between mouse and cricket under 1.6 cm. I then defined an approach as time at which the azimuth between mouse and cricket was between -90 and 90 degrees, mouse velocity above .2cm per second, cricket velocity under .12cm/second and range steadily decreasing at minimum $-.2$ cm per second. Then a pursuit was defined as cricket velocity over .12cm per second, mouse velocity must be greater than cricket velocity as well as a change in range under 0 cm per second. A flight was the characterized as cricket velocity over .12cm per second, cricket velocity must be greater than mouse velocity as well as a change in range over 0 cm per second. A freeze is defined as mouse velocity under 2 cm per second. Finally, explore was defined as cricket velocity over .12 cm per second, and mouse velocity must be greater than cricket velocity. Each syllable is defined in this specific order, to filter the syllables appropriately.

Results

Hunting comprises several behavioural syllables

I applied standard methods to train mice in a visually guided prey capture assay and filmed the movement of cricket and mouse over a 5-minute trial. Videos were labelled using DeepLabCut (**Figure 1A-C**) to obtain nose, ear, and tail positions for the mouse and the body cricket position. These markers were used to compute mouse-cricket distance (range), mouse-cricket angle (azimuth), and mouse-cricket velocity. Like prior studies, mice achieved peak performance within 7-10 days as judged by the probability of capture and average capture time (**Figure 1E**). I noticed that mouse behaviour within hunting trials often showed repeated features. To quantify this, I defined a series of sub-behaviours,

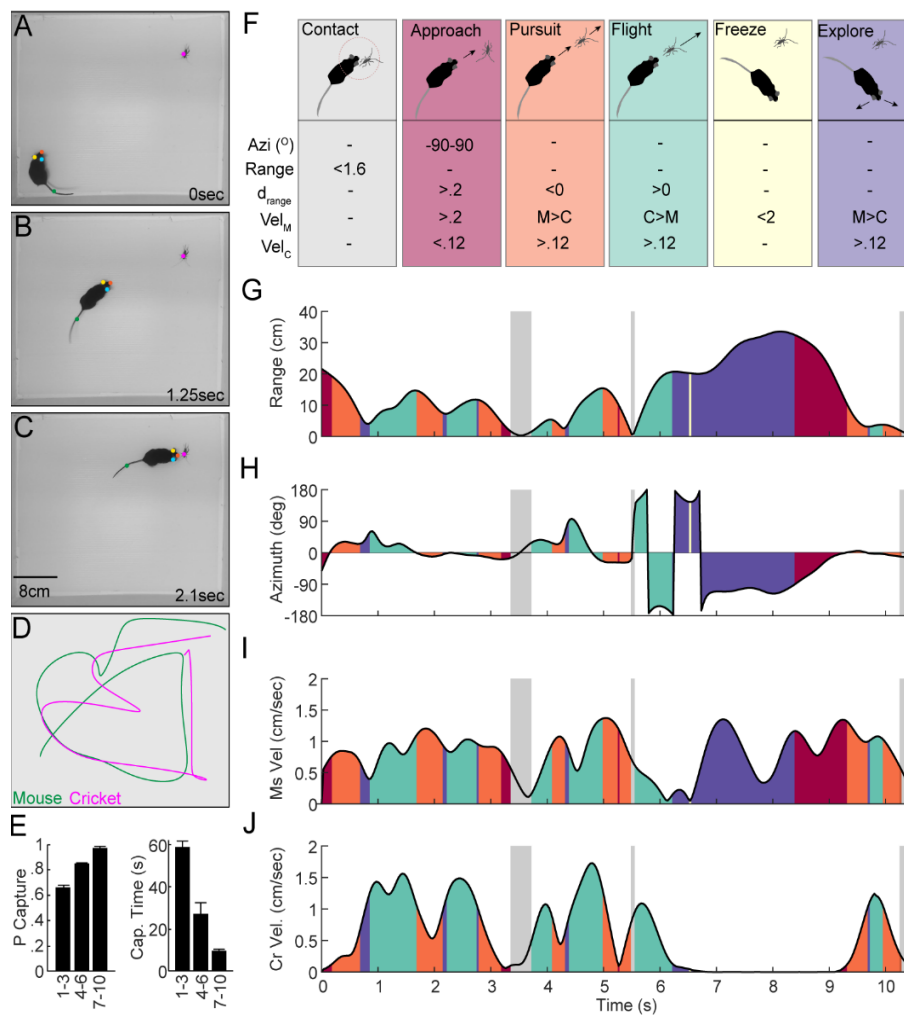


Figure 1. Prey capture comprises several behavioural syllables.

A-C. Sample frames taken from a hunt showing mouse, cricket, and DLC labeling of the ears, nose, tail, and cricket. **D.** Mouse and cricket tracks taken from the markers shown in A. **E.** Average probability of capture and time to capture across days. **F.** Cartoons depict 6 sub-behaviors we term “syllables” as well as the azimuth (Azi), change in range (DRange), mouse velocity (Vel_M), and cricket velocity (Vel_C) parameters used to define them. **G-J.** Plot of range versus time (G), azimuth versus time (H), mouse velocity (I), and cricket velocity (J) from an example hunting trial. **G-J.** Plot of range versus time (G), azimuth versus time (H), mouse velocity (I), and cricket velocity (J) from an example hunting trial.

which I term syllables, using a set of criterion values for range, azimuth, and animal velocities (see methods). I define six syllables: contact, approach, pursuit, flight, freeze, and explore (**Figure 1F-G**) and propagated their labels across our trial data to observe their spatial and temporal structure. Syllables often repeat across a trial and appeared to follow one another in stereotyped sequences. This observation led me to analyze the spatial and temporal structure of syllables across hunting trials.

Hunting Syllables are initiated at specific mouse and cricket spatiotemporal arrangements.

I next binned (2cm) mouse nose and cricket positions over the arena for every trial and examined their distribution. Mouse and cricket often preferred the edges of the arena rather than the middle (**Figure 2A-B**), consistent with the tendency of these animals to avoid open spaces. However, when I subdivided this data into syllables and considered their position, I saw major differences with this overall pattern.

During approaches, mice were often in the center of the arena with crickets sitting along the walls or in the corners (**Figure 2C**). Pursuits resembled approaches but showed the mice at a more wall-proximate position (**Figure 2D**). Contacts occurred primarily in the corners, suggesting a strategy of pinning crickets to corners to enhance the chance of capture (**Figure 2E**). Flights looked like inverted approaches with mice in the corners and walls and crickets in the center of the box (**Figure 2F**), consistent with the ballistic jumps

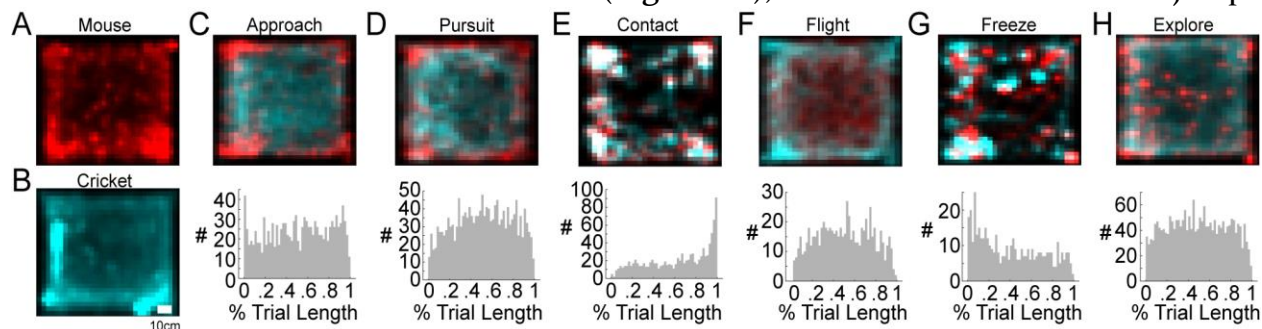


Figure 2. Spatial and temporal structure of hunting syllables. A-B. 2D histogram of mouse (A) and cricket (B) position across all trials between hunting days 7-10. C-H. 2D histograms of mouse and cricket position (top) during approach (C), pursuit (D), contact (E), flight (F), freeze (G), and explore (H) syllables and a corresponding histogram of syllable initiation over normalized trial length.

that the crickets use to evade capture. Freezes syllables showed focal spots for both mouse and cricket that were distributed throughout the arena, whereas explore syllables showed

mice all throughout the arena (**Figure 2H**). Binning syllable onset over normalized trial length showed that approaches, pursuits, flights, and explores could occur at any time within a trial (**Figure 2C-H**). Contacts which were often enriched at the end of trial (**Figure 2E**) and freezes were often enriched in the beginning of a trial (**Figure 2G**) consistent with our observation that mice ‘spot’ the cricket and then take a few attempts before capturing their prey.

Taken together, these data show that hunting behaviour consists of an underlying structure composed of discrete behavioural syllables which correlate with specific spatiotemporal arrangements of mouse-cricket.

Syllable transitions are highly non-random and form distinct sequences.

Given this spatial arrangement I next considered how mice transition from syllable to the next. To do this, I obtained a vector of syllable labels for the length of each trial and computed the transition probability from any given syllable into all syllables (**Figure 3A**). Internal transition probabilities (ie: approach→approach or explore→explore) were significantly higher than external transition probabilities, consistent with the idea that syllables are bona fide sub-behaviours of hunting. To resolve the structure of these transition probabilities, I visualized this matrix using a directed Markov chain graph which positions syllables in the x-y plane according to the probability that they transition into themselves (**Figure 3B**). This visualization confirmed several observed features of hunting behaviour. One wing of this representation, which I term the hunting sequence, comprises explore, approach, pursuit, contact and capture syllables (**Figure 3C**). Another, which I term the ‘idle’ sequence, comprised explore and freeze syllables (**Figure 3C**). Trained mice often interleaved hunting and idle sequences for up to 2-3 cycles prior to a capture. Weaker connections were observed between freeze→pursuit syllables, freeze→contact, flight→contact and flight→freeze syllables (**Figure 3B**). Taken together, these data show that mice execute a stereotyped sequence of behavioural syllables after 7-10 days of hunting which correlates with peak performance. Given that the probability of capture and average

capture time evolves over ~7days and given the weaker connections between states such as flight and freeze at 7days, I next asked how hunting and idle sequences evolve over training.

Inter-syllabic transition probabilities evolve with training

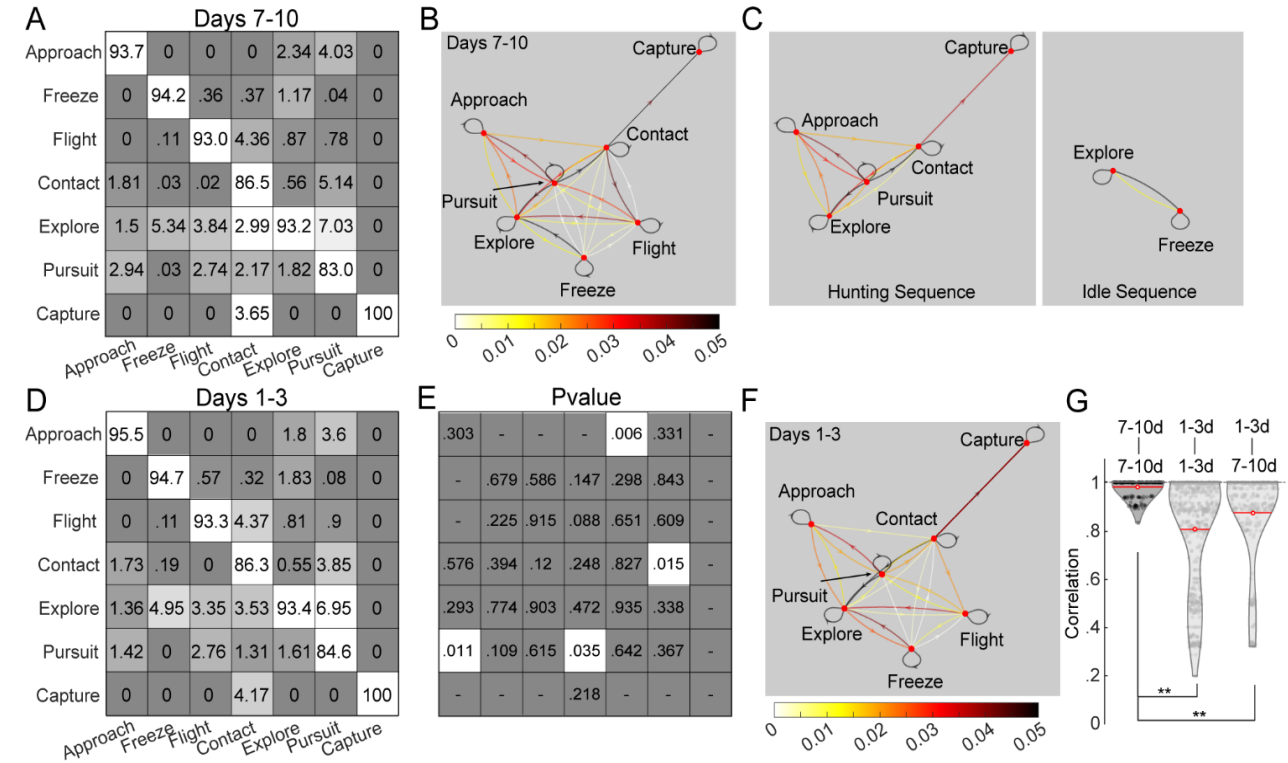


Figure 3. Inter-syllabic transition probability. **A.** Average syllable-syllable transition probability for 16 mice over days 7-10. **B.** Directed markov chain graph visualizing the data shown in A. **C.** The same directed graph dissected into a hunting and idle sequence. **D.** Average syllable-syllable transition probability for 16 mice over days 1-3. **E.** P-values from a 1-way anova test between each cell of the transition probability matrices shown in A and D. **F.** Directed markov chain graph visualizing the data shown in A. **G.** pairwise correlation between transition probability matrices for each mouse at 7-10 days, 1-3 days, and between 1-3 days and 7-10 days of hunting. High correlations among 7-10 data indicate a common inter-syllabic structure. Lower correlation scores among 1-3 data indicate differing intersyllabic structure on the first few days of hunting. Mice on day 1-3 show a different inter-syllabic structure than mice at 7-10.

Visualizing transition probability matrices for the first 3 days of hunting showed a Markov chain with a similar gross structure as that seen at days 7-10 (Figure 3D-E). However, there were key differences: First, I noted that connections between syllables in the hunting sequence such as explore→approach, approach→pursuit, contact→pursuit, and pursuit→contact were significantly different at days 1-3 versus days 7-10 (Figure 3E). Second, I noticed that the connection between explore→freeze, which maintains the idle

sequence were stronger at days 1-3, but these differences were not statistically different (**Figure 3D&F**). Finally, I quantified the similarity of transition probability matrices from individual mice at a given time point by vectorizing these matrices and computing pairwise correlations. As expected, matrices computed from individual mice at days 7-10 were highly correlated with the matrices of mice from the same time point (**Figure 3G**). Matrices obtained on day 1-3 showed weaker correlations with mice at the same time point and significantly weaker than those computed from mice at days 7-10 (**Figure 3G**), consistent with the notion that mice need a few days to find the ideal hunting strategy. These results indicate that the structural changes seen in our Markov chain diagrams reflect changes in hunting strategy across training. Thus, mice display the basic hunting sequence on the first day in the arena but selectively strengthen or weaken inter-syllabic connections as performance improves.

Syllable transitions that lead to capture occur at a specific range, azimuth, and velocity

Given that mice strengthen some syllabic transitions and weaken others over training, I next asked whether the syllable transitions that lead to capture occur at a specific range, azimuth, and cricket velocity. To do this, I examined the distribution of these parameters extracted from a 5-frame period just prior to each kind of syllable transition (**Figure 4A-C**).

This analysis showed several interesting features. First, explores that convert into approaches often begin at a range ~30cm and have a stationary cricket sitting squarely within the monocular visual field (**Figure 4A**). Second, approach→pursuit transitions begin at a range of ~20cm, or two mouse body-lengths, and have a stationary cricket at the edge of the binocular zone (**Figure 4B**). Third, pursuit to contact transitions happen at a range of <15cm and have a moving cricket well within the binocular zone (**Figure 4C**).

Reversions at each of these steps showed statistically significant differences in the azimuthal position of the cricket. For example, approaches that convert back into explores

occur at a somewhat higher range and azimuth as compared to those that convert into pursuits (Figure 4D), suggesting that the mouse simply could not bring the cricket into the binocular region. As another example, pursuits convert into approaches or explores show higher azimuths but comparable ranges (Figure 4E), suggesting the mouse simply cannot maintain its prey within the binocular zone. Taken together, these results indicate that conversion from explore→approach→pursuit→contact involves the mouse side-eyeing the cricket and narrowing the distance to its prey, while simultaneously centering the cricket within the binocular visual field.

Chemogenetic silencing or ablation of RGC types impairs different aspects of hunting.

I next asked whether specific RGC types inform syllable transitions within the hunting sequence. I focused on two RGC classes, a set of RGCs selective to directional motion (DSGCs) and a set of RGCs that encode stationary bright and dark objects (α RGCs). Recent studies implicate signals from both kinds of RGCs in visually guided predation but a direct test of their contribution to hunting and their impact on syllabic transitions has not been performed.

To address this idea, I selectively impaired SACs whose signals are essential for the DS responses of all retinal DSGCs, or selectively impaired α RGCs using chemogenetic tools and studied the impact of these manipulations on hunting. I then compared the results of these experiments to results obtained by selectively inhibiting a random assortment of RGC

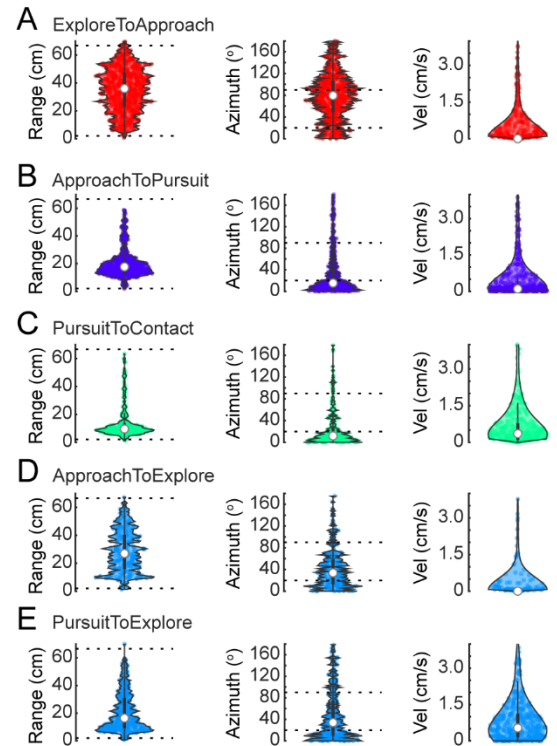


Figure 4. Cricket position and velocity prior to syllable transitions. A-E. Violin plots showing the range (left), azimuth (middle), and velocity (right) over 5 frames just prior to an explore→approach (A), approach→pursuit (B), pursuit→contact (C), approach→explore (D), and pursuit→explore (E) transitions.

types. Our expectation was that impairment of α RGC and DSGCs would show selective effects on hunting syllable structure and be different from perturbation of all RGCs.

To do this I intraocularly injected mice that grant genetic access to starbursts (ChAT-Cre), α RGCs (KCNG4-Cre), or all RGCs (VGlut2-Cre) with AAVs bearing Cre-dependent constructs encoding the inhibitory DREADD, HM4Di. Next, I trained these animals to hunt prey for 7-10 days and then applied CNO prior to hunting trials on each subsequent day to examine effects. A subset of mice was infected with AAVs bearing Cre-Dependent diphtheria toxin receptor, injected with diphtheria toxin after 7-10 days of training, and then assessed for an additional week. I obtained similar results with both methods and have pooled these datasets together below.

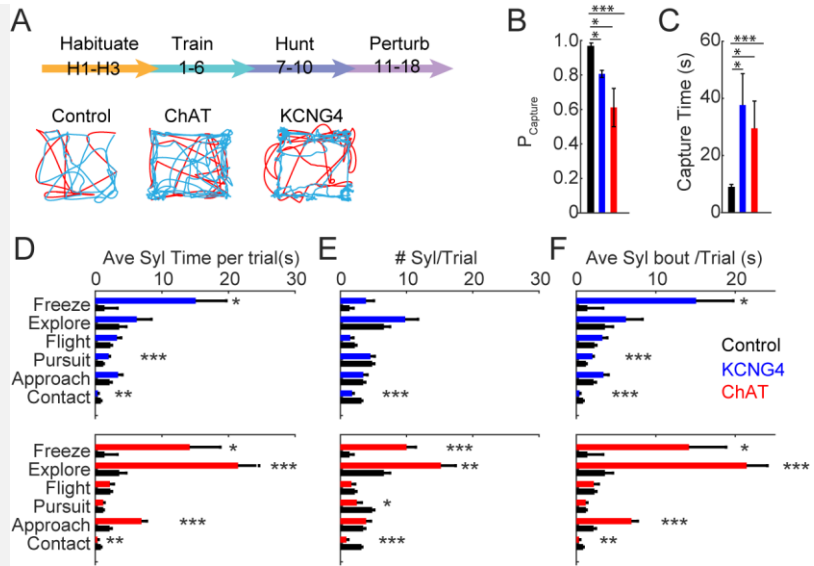
Chemogenetic disruption of RGCs labelled in all three lines impaired hunting that was evident on a single trial (**Figure 5A**) and led to a significant reduction in the average capture probability and capture time (**Figure 5B-C**). I next analyzed the syllabic composition of hunts in each line and compared this composition to that obtained in controls. Chemogenetic inhibition within each Cre line produced both common and differential effects on syllable structure. All lines showed a decrease in the number of contacts and their average duration per trial (**Figure 5E-F**), consistent with the overall reduction in P_{capture} . Changes to the approach, pursuit, flight, explore, or freeze syllables varied according to Cre line.

Chemogenetic inhibition in the Vglut2-Cre line led to significant, but modest, increases to the length of pursuits. Increases to freeze and explore syllable length were also observed, but these changes were not statistically significant. No change in the number of syllables, other than contacts, was observed. Thus, perturbation of a random assortment of RGC types leads mice to have fewer contacts with slightly more pursuits.

The same perturbation in the KCNG4-Cre line led to different results. Chemogenetic perturbation did not alter the number of each syllable per trial but led to a significant lengthening in pursuit and freeze syllables (**Figure 5E-F**), suggesting that the loss of α RGCs leads mice to longer pursuits punctuated by very long freezes.

Figure 5. Chemogenetic disruption of RGCs impairs hunting and disrupts syllabic structure.

A. Schematic of the hunting schedule showing habituation (3 days), training (3 days), hunting (3 days), and perturbation (3-7 days). **B-C.** Average probability of capture (B) and Capture time (C) computed from trained control mice (Black) and trained KCNG4-Cre (Blue), ChAT-Cre, and Vglut2-Cre mice after chemogenetic disruption. **D-F.** Average total time spent in the indicated syllables per trial (E), average number of syllables per trial, and average syllable length



(G) computed from trained control mice (n=30) and chemogenetically treated KCNG4-Cre mice (n=5), ChAT-Cre (n=6), and Vglut2-Cre (n=6) mice following chemogenetic perturbation. Bars show mean +/- SEM, * = P<.05, ** = P<.01, *** = P<.001.

Results with ChAT-Cre lines differed from both Vglut2- and KCNG4-Cre lines. Perturbation studies in this line significantly decreased the number of pursuits and increased the number of freeze and explore syllables (Figure 5E-F). Explore and freeze syllables were also significantly longer than their control counterparts (Figure 5F). Taken together, these results suggest that perturbing SACs leads mice to execute more freeze and explore syllables and stay within these syllables for longer than their control counterparts.

Thus, disruption of DSGCs and α RGCs produced different effects on hunting syllable structure that differed from broad disruption of all RGCs. Given these results I next analyzed intersyllabic transitions within these three perturbation experiments.

Perturbation of DSGCs or α RGCs impairs different hunting syllable transitions

Markov chain diagrams computed from hunts with disrupted α RGC and DSGCs were visibly different from each other and from controls (Figure 6A-C). Mice belonging to either α RGC- and DSGC-disrupted groups showed transition probability matrices showed relatively high correlation to their group and lower correlation with the matrices from controls (Figure 6D). These observations support the idea that loss of either RGC type produces consistent changes in the behavioural structure of hunting. Statistical

comparison of each syllable transition between controls and RGC-perturbed mice showed that loss of α RGCs and DSGCs affected different syllable transitions (**Figure 6E-F**).

Perturbing α RGCs lowered approach→approach, contact→contact, and contact→capture probabilities and increased contact→explore and pursuit→approach probabilities (**Figure 6E**). These changes would have the effect of reversing the hunting sequence, moving mice from the contact syllable back towards approach (**Figure 6B**). The same experiment in ChAT-Cre mice affected different syllables. Here, only approach→approach probability was elevated (**Figure 6F**), consistent with the longer approaches I measured in this group. Transitions involving approach→contact, approach→pursuit, contact→capture, contact→contact, and pursuit→contact probabilities were all significantly weaker (**Figure 6F**). Thus, loss of DSGCs weakens the forward movement through the hunting sequence which leads to contact and therefore capture. Finally, I considered the range and azimuth at each of these affected syllabic transitions to see if the sensory stimulus (cricket) prior to syllable transitions differs from controls.

Perturbation of DSGC or α RGCs alters the range and azimuth at which syllables are initiated

Mice with disrupted α RGCs showed significant re-organization in the range and azimuth at which syllables were initiated. Crickets were positioned at azimuths and ranges prior to Approaches→approach α RGCs-perturbed mice that would normally lead to approach→pursuit conversions. The same trend is seen in contact→contact transitions which have the cricket central azimuths that typically precede contact→capture transitions. Pursuit→approach and pursuit→flight transitions both occurred at ranges that should lead to contact but in α RGC-disrupted mice do not. Explore→approach transitions occurred at closer ranges than their control counterparts.

The situation with ChAT-Cre perturbations is more complex. Disruption in these lines led to smaller alterations in the azimuth at which affected syllable transitions occurred. There was too few approach→contact transitions to analyze cricket position in mice with disrupted DSGCs indicating that their absence prevents this syllabic transitions.

The same animals Approaches → pursuit transitions at much longer ranges. I interpret these data as the mouse being unable to sneak up on the cricket as well as their control counterparts.

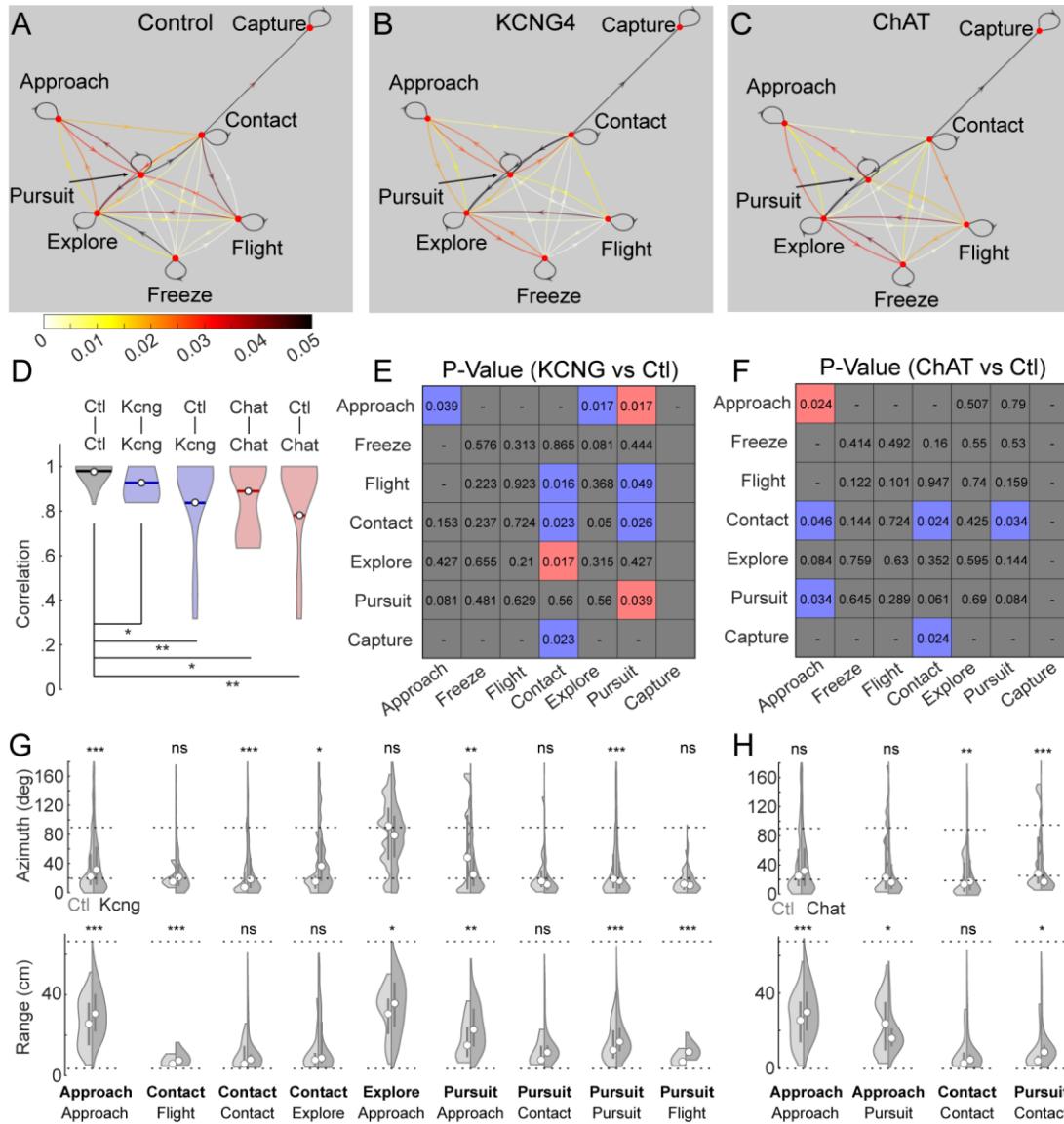


Figure 6. **A-C.** Directed Markov chain graphs computed from transition matrices in controls (A), in mice with perturbed aRGCs (B) or DSGCs (C). Violin plots of correlations computed within controls (ctl-ctl), perturbed aRGCs (kcng-kcng), perturbed DSGCs (Chat-Chat), and between these perturbation conditions and controls (ctl-kcng and ctl-Chat). **E-F.** Matrices of p-values computed from comparing transition probability matrices from mice with perturbed aRGCs (E) and DSGCs (F). Colors indicate whether probability in perturbation is higher (red) or lower (blue) than controls. **G-H.** Split violin plots showing azimuth and range in the 5 frames prior to the indicated syllable transitions in mice with perturbed aRGCs (G) or DSGCs (H) as compared to controls. Syllable transitions are the statistically different ones shown in E-F.

Contacts show a small but significant reduction in the azimuth at which they occur and pursuits converting into contacts now occur at shorter distances and at more lateral positions in azimuth. These deficits are somewhat hard to interpret but could be consistent with an inability of the mouse to detect motion at short range. Thus, disrupting DSGCs leads mice to initiate syllable transitions at shorter ranges than their control counterparts.

Discussion

Here, I used an innate prey-capture assay to examine the contribution of two RGC types upon a visually guided behaviour. Using behavioural analysis, I discovered that hunting is composed of seven sub-behaviours: approach, pursuit, contact, freeze, flight, explore and capture. Such sub-behaviours were highly stereotyped across individual mice and their specific sequence developed over the 1 week it takes mice to learn this task. Syllables were often initiated at specific mouse-cricket distances (range) and azimuthal positions. Next, I analyzed the consequences of perturbing α GCs and DSGCs on hunting syllable structure and hunting performance. I learned that disruption of RGCs in both lines impaired hunting and led to a significant decrease in capture probability and increase in capture time. Syllabic analysis showed a specific loss of approach and contact continuity, reduced contact→capture but increased contact→explore probabilities in mice with perturbed α RGCs. In mice with perturbed DSGCs, I observed longer approaches, with weakened approach→contact/pursuit probabilities as well as contact→capture/contact probabilities. Finally, I examined the position of crickets just prior to syllable initiation and found that mice with perturbed DSGCs significantly altered the angle and distance to crickets at which they initiated syllables, increasing range and azimuth. Mice with perturbed α RGCs were unable to stalk prey successfully, needing to initiate syllable transitions at a shorter distance to the cricket. Taken together, these data show that these two RGC types contribute to distinct aspects of prey capture. These data suggest that the remaining RGC types could contribute similarly.

Hunting comprises several behavioural syllables

I identified a highly stereotyped non-random sequence of behavioural syllables that make up a hunt. Such hunting sequences usually comprised of an explore, approach, pursuit, freeze, flight, contact and capture syllable, while idle sequences were comprised of freezes and explores. Further examining the transitions between syllables, transitions between sequences were established within the first few days, but certain transitions strengthen or weaken as the mouse develops its strategy over 7-10 days. Transition between these variables rely on strategy, but also occur at specific ranges and azimuths. Explores turns into approaches when the cricket is around 30 cm and in the monocular zone, which turns into pursuits when the cricket is 20 cm and on the edge of the binocular zone, and finally turning into contacts when the mouse is within 15 cm and in the binocular zone. Therefore, the mouse explores until it sees a cricket, will start pursuing and orienting the cricket in their binocular zone while reducing the distance between them.

RGC loss compromises specific syllable transitions

Mice saw a general increase in capture time and decrease in capture probability when their RGCs were chemogenetically silenced. Silencing a random assortment of RGCs in Vglut2-Cre mice resulted in longer pursuit sequences and fewer contact sequences. Silencing all α RGC in KCNG4-Cre mice led to significantly longer pursuit and freeze syllables, as well as modifying the azimuth and range at which they transition between syllables. Perturbation of SACs in ChAT-Cre mice resulted in decreased numbers of pursuits but increased both the number and the length of freeze and explore syllables. Mice tend to transition between syllables at a shorter range, being unable to initiate long-range sequences.

RGCs and visual guided behaviours

These findings are consistent with previous studies that studied the relationship between RGCs and behaviour. Ablation of some RGC can lead to modification in behavioural syllables, there is impaired escape and freezing syllables during looming tasks

when ablating w_3 tOFF α RGCs in mice (Wang et al., 2021). My results add and expand to this conclusion.

It was shown that when mice hunt, they keep the prey image on a small area of the retina where the vestibular ocular reflex stabilizes the visual field. And this area has minimal optic flow which permits for decreased motion induced blur (Holmgren et al., 2021). This coincides with the region with the highest density of α RGCs which is also located in the ipsilateral zone, also known as the binocular zone. α RGCs are looking for bright or dark objects located within the binocular zone. When chemogenetically silencing α RGCs during prey capture, the mice tend to modify their azimuths during approach, and have longer pursuit and freeze syllables. It seems like the mice have a harder time getting the cricket within the binocular zone and keeping it there until successful capture. This would in turn affect the mouse's OKR further impairing their hunting abilities.

DSGCs are looking for bright or dark objects or edges across the visual field. When DS cells are selectively ablated, zebrafish lack orienting behaviour (Gahtan, 2005), and deficits of DS neurons in V_1 disrupts optic flow (Morrie & Feller, 2017). Furthermore, when Hoy et al. (2019) ablated DS cells in SC, mice had decreased accurate orienting behaviour and had trouble maintaining continuous approaches. This seems to be consistent with my findings in which starburst amacrine direction selective cells are silenced. Mice had longer and more numerous freezes and explore syllables, and transitions were done at a shorter range due to lack of continuous approaches. Mice had a harder time noticing the cricket, and once noticed the mice tended to abort the hunt prematurely, perhaps due to lack of direction perception. DS cells are also responsible for partially mediating the optokinetic reflex and the vestibular ocular reflex, both crucial for gaze stabilizing, and ablating SAC results in heavy deficits of the OKR (Yonehara et al., 2009; K. Yoshida et al., 2001). Silencing DS cells may have reduced mouse reflex on a similar but smaller scare compared to when silencing α RGCs, whose cell density corresponds with gaze stabilizing neurons (Holmgren et al., 2021). This will also affect continuous approaches, which I noticed in my findings.

Behavioural syllables

Wiltschko et al. (2015) developed methods combining 3d imaging with machine learning, creating a model of mouse behaviour, which shows that behaviour is composed of highly stereotyped and repeated syllables with defined transition probability, all happening at the sub-second time scale. This offers the possibility of looking at both internal (contact to contact) and external (contact to catch) syllabic transitions with precision that is not possible on the human scale. This method offers insight for both predicted and spontaneously appearing phenotypes and how these may be disrupted syllable sequence using chemogenetic manipulations. External environmental influences could also be analysed, to better understand how the mice react to its surrounding. Repeating my experiments using the methods of Wiltschko et al. offer a tractable way to address syllable transitions and all their subtleties.

Conclusion

Mice hunt prey in a stereotypical way and perturbing certain RGCs can significantly impair this hunting sequences. Hunting behaviour can be deconstructed into 6 different syllables whose inter-syllable transitions strengthen within the first 10 days. Disrupting either direction selective RGCs in ChAT-Cre mice and α RGC in KCNG4-Cre impairs specific inter-syllable sequences which in turn impairs the overall hunting sequence. This information serves to further expand our understanding on how certain RGCs affect behaviour, and the way they do so. Ablating certain RGC show that these are responsible for guiding specific moments in behaviour rather than the whole behaviour itself.

References

- Baden, T., Berens, P., Franke, K., Román Rosón, M., Bethge, M., & Euler, T. (2016). The functional diversity of retinal ganglion cells in the mouse. *Nature*, *529*(7586), 345–350. <https://doi.org/10.1038/nature16468>
- Bleckert, A., Schwartz, G. W., Turner, M. H., Rieke, F., & Wong, R. O. L. (2014). Visual space is represented by non-matching topographies of distinct mouse retinal ganglion cell types. *Current Biology : CB*, *24*(3), 310–315. <https://doi.org/10.1016/j.cub.2013.12.020>
- Boycott, B. B., & Wässle, H. (1974). The morphological types of ganglion cells of the domestic cat's retina. *The Journal of Physiology*, *240*(2), 397–419. <https://doi.org/10.1113/jphysiol.1974.sp010616>
- Cang, J., Savier, E., Barchini, J., & Liu, X. (2018). Visual Function, Organization, and Development of the Mouse Superior Colliculus. *Annual Review of Vision Science*, *4*(1), 239–262. <https://doi.org/10.1146/annurev-vision-091517-034142>
- Carter-Dawson, L. D., & Lavail, M. M. (1979). Rods and cones in the mouse retina. I. Structural analysis using light and electron microscopy. *Journal of Comparative Neurology*, *188*(2), 245–262. <https://doi.org/10.1002/cne.901880204>
- Chen, J. W., Gombart, Z. J., Rogers, S., Gardiner, S. K., Cecil, S., & Bullock, R. M. (2011). Pupillary reactivity as an early indicator of increased intracranial pressure: The introduction of the Neurological Pupil index. *Surgical Neurology International*, *2*, 82. <https://doi.org/10.4103/2152-7806.82248>

- Chen, P., & Hong, W. (2018). Neural Circuit Mechanisms of Social Behavior. *Neuron*, 98(1), 16–30. <https://doi.org/10.1016/j.neuron.2018.02.026>
- Crawley, J. N. (2007). *Social Behavior Tests for Mice*. 8.
- Cruz-Martín, A., El-Danaf, R. N., Osakada, F., Sriram, B., Dhande, O. S., Nguyen, P. L., Callaway, E. M., Ghosh, A., & Huberman, A. D. (2014). A dedicated circuit linking direction selective retinal ganglion cells to primary visual cortex. *Nature*, 507(7492), 358–361. <https://doi.org/10.1038/nature12989>
- de Malmazet, D., Kühn, N. K., & Farrow, K. (2018). Retinotopic Separation of Nasal and Temporal Motion Selectivity in the Mouse Superior Colliculus. *Current Biology*, 28(18), 2961–2969.e4. <https://doi.org/10.1016/j.cub.2018.07.001>
- Demb, J. B. (2007). Cellular mechanisms for direction selectivity in the retina. *Neuron*, 55(2), 179–186. <https://doi.org/10.1016/j.neuron.2007.07.001>
- Dhande, O. S., Estevez, M. E., Quattrochi, L. E., El-Danaf, R. N., Nguyen, P. L., Berson, D. M., & Huberman, A. D. (2013). Genetic Dissection of Retinal Inputs to Brainstem Nuclei Controlling Image Stabilization. *Journal of Neuroscience*, 33(45), 17797–17813. <https://doi.org/10.1523/JNEUROSCI.2778-13.2013>
- Dunn, F. A., Doan, T., Sampath, A. P., & Rieke, F. (2006). Controlling the Gain of Rod-Mediated Signals in the Mammalian Retina. *Journal of Neuroscience*, 26(15), 3959–3970. <https://doi.org/10.1523/JNEUROSCI.5148-05.2006>
- Euler, T., Detwiler, P. B., & Denk, W. (2002). Directionally selective calcium signals in dendrites of starburst amacrine cells. *Nature*, 418(6900), 845–852. <https://doi.org/10.1038/nature00931>

- Euler, T., Haverkamp, S., Schubert, T., & Baden, T. (2014). Retinal bipolar cells: Elementary building blocks of vision. *Nature Reviews Neuroscience*, *15*(8), 507–519. <https://doi.org/10.1038/nrn3783>
- Euler, T., & Masland, R. H. (2000). Light-Evoked Responses of Bipolar Cells in a Mammalian Retina. *Journal of Neurophysiology*, *83*(4), 1817–1829. <https://doi.org/10.1152/jn.2000.83.4.1817>
- Gahtan, E. (2005). Visual Prey Capture in Larval Zebrafish Is Controlled by Identified Reticulospinal Neurons Downstream of the Tectum. *Journal of Neuroscience*, *25*(40), 9294–9303. <https://doi.org/10.1523/JNEUROSCI.2678-05.2005>
- Gauvain, G., & Murphy, G. J. (2015). Projection-Specific Characteristics of Retinal Input to the Brain. *Journal of Neuroscience*, *35*(16), 6575–6583. <https://doi.org/10.1523/JNEUROSCI.4298-14.2015>
- Goetz, J., Jessen, Z. F., Jacobi, A., Mani, A., Cooler, S., Greer, D., Kadri, S., Segal, J., Shekhar, K., Sanes, J. R., & Schwartz, G. W. (2022). Unified classification of mouse retinal ganglion cells using function, morphology, and gene expression. *Cell Reports*, *40*(2), 111040. <https://doi.org/10.1016/j.celrep.2022.111040>
- Gollisch, T., & Meister, M. (2010). Eye smarter than scientists believed: Neural computations in circuits of the retina. *Neuron*, *65*(2), 150–164. <https://doi.org/10.1016/j.neuron.2009.12.009>
- Grimes, W. N., Zhang, J., Graydon, C. W., Kachar, B., & Diamond, J. S. (2010). Retinal Parallel Processors: More than 100 Independent Microcircuits Operate within a

Single Interneuron. *Neuron*, 65(6), 873–885.

<https://doi.org/10.1016/j.neuron.2010.02.028>

- Hatori, M., Le, H., Vollmers, C., Keding, S. R., Tanaka, N., Buch, T., Waisman, A., Schmedt, C., Jegla, T., & Panda, S. (2008). Inducible ablation of melanopsin-expressing retinal ganglion cells reveals their central role in non-image forming visual responses. *PloS One*, 3(6), e2451. <https://doi.org/10.1371/journal.pone.0002451>
- Holmgren, C. D., Stahr, P., Wallace, D. J., Voit, K.-M., Matheson, E. J., Sawinski, J., Bassetto, G., & Kerr, J. N. (2021). Visual pursuit behavior in mice maintains the pursued prey on the retinal region with least optic flow. *ELife*, 10, e70838. <https://doi.org/10.7554/eLife.70838>
- Hoy, J. L., Bishop, H. I., & Niell, C. M. (2019). Defined Cell Types in Superior Colliculus Make Distinct Contributions to Prey Capture Behavior in the Mouse. *Current Biology*, 29(23), 4130–4138.e5. <https://doi.org/10.1016/j.cub.2019.10.017>
- Hoy, J. L., Yavorska, I., Wehr, M., & Niell, C. M. (2016). Vision Drives Accurate Approach Behavior during Prey Capture in Laboratory Mice. *Current Biology*, 26(22), 3046–3052. <https://doi.org/10.1016/j.cub.2016.09.009>
- Huberman, A. D., Manu, M., Koch, S. M., Susman, M. W., Lutz, A. B., Ullian, E. M., Baccus, S. A., & Barres, B. A. (2008). Architecture and activity-mediated refinement of axonal projections from a mosaic of genetically identified retinal ganglion cells. *Neuron*, 59(3), 425–438. <https://doi.org/10.1016/j.neuron.2008.07.018>

- Ito, S., & Feldheim, D. A. (2018). The Mouse Superior Colliculus: An Emerging Model for Studying Circuit Formation and Function. *Frontiers in Neural Circuits*, 12. <https://www.frontiersin.org/articles/10.3389/fncir.2018.00010>
- Ito, S., Feldheim, D. A., & Litke, A. M. (2017). Segregation of Visual Response Properties in the Mouse Superior Colliculus and Their Modulation during Locomotion. *The Journal of Neuroscience*, 37(35), 8428–8443. <https://doi.org/10.1523/JNEUROSCI.3689-16.2017>
- Jeon, C.-J., Strettoi, E., & Masland, R. H. (1998). The Major Cell Populations of the Mouse Retina. *The Journal of Neuroscience*, 18(21), 8936–8946. <https://doi.org/10.1523/JNEUROSCI.18-21-08936.1998>
- Johnson, K. P., Fitzpatrick, M. J., Zhao, L., Wang, B., McCracken, S., Williams, P. R., & Kerschensteiner, D. (2021). Cell-type-specific binocular vision guides predation in mice. *Neuron*, 109(9), 1527–1539.e4. <https://doi.org/10.1016/j.neuron.2021.03.010>
- Johnson, V. G., Wilson, D., Greenfield, L., & Youle, R. J. (1988). The role of the diphtheria toxin receptor in cytosol translocation. *Journal of Biological Chemistry*, 263(3), 1295–1300. [https://doi.org/10.1016/S0021-9258\(19\)57299-4](https://doi.org/10.1016/S0021-9258(19)57299-4)
- Kay, J. N., De la Huerta, I., Kim, I.-J., Zhang, Y., Yamagata, M., Chu, M. W., Meister, M., & Sanes, J. R. (2011). Retinal Ganglion Cells with Distinct Directional Preferences Differ in Molecular Identity, Structure, and Central Projections. *Journal of Neuroscience*, 31(21), 7753–7762. <https://doi.org/10.1523/JNEUROSCI.0907-11.2011>
- Kerschensteiner, D. (2022). Feature Detection by Retinal Ganglion Cells. *Annual Review of Vision Science*, 8(1), null. <https://doi.org/10.1146/annurev-vision-100419-112009>

- Kim, T., Shen, N., Hsiang, J.-C., Johnson, K. P., & Kerschensteiner, D. (2020). Dendritic and parallel processing of visual threats in the retina control defensive responses. *Science Advances*, 6(47), eabc9920. <https://doi.org/10.1126/sciadv.abc9920>
- Krauzlis, R. J., Lovejoy, L. P., & Zénon, A. (2013). Superior Colliculus and Visual Spatial Attention. *Annual Review of Neuroscience*, 36, 10.1146/annurev-neuro-062012-170249. <https://doi.org/10.1146/annurev-neuro-062012-170249>
- Krieger, B., Qiao, M., Rouso, D. L., Sanes, J. R., & Meister, M. (2017). Four alpha ganglion cell types in mouse retina: Function, structure, and molecular signatures. *PLOS ONE*, 12(7), e0180091. <https://doi.org/10.1371/journal.pone.0180091>
- Krishnaswamy, A., Yamagata, M., Duan, X., Hong, Y. K., & Sanes, J. R. (2015). Sidekick 2 directs formation of a retinal circuit that detects differential motion. *Nature*, 524(7566), 466–470. <https://doi.org/10.1038/nature14682>
- Langley, W. M. (1989). Grasshopper mouse's use of visual cues during a predatory attack. *Behavioural Processes*, 19(1), 115–125. [https://doi.org/10.1016/0376-6357\(89\)90035-1](https://doi.org/10.1016/0376-6357(89)90035-1)
- Liu, B., Huberman, A. D., & Scanziani, M. (2016). Cortico-fugal output from visual cortex promotes plasticity of innate motor behaviour. *Nature*, 538(7625), 383–387. <https://doi.org/10.1038/nature19818>
- Lolley, R. N., & Lee, R. H. (1990). Cyclic GMP and photoreceptor function. *The FASEB Journal*, 4(12), 3001–3008. <https://doi.org/10.1096/fasebj.4.12.1697545>
- MacNeil, M. A., & Masland, R. H. (1998). Extreme Diversity among Amacrine Cells: Implications for Function. *Neuron*, 20(5), 971–982. [https://doi.org/10.1016/S0896-6273\(00\)80478-X](https://doi.org/10.1016/S0896-6273(00)80478-X)

- Macosko, E. Z., Basu, A., Satija, R., Nemes, J., Shekhar, K., Goldman, M., Tirosh, I., Bialas, A. R., Kamitaki, N., Martersteck, E. M., Trombetta, J. J., Weitz, D. A., Sanes, J. R., Shalek, A. K., Regev, A., & McCarroll, S. A. (2015). Highly Parallel Genome-wide Expression Profiling of Individual Cells Using Nanoliter Droplets. *Cell*, *161*(5), 1202–1214. <https://doi.org/10.1016/j.cell.2015.05.002>
- Manvich, D. F., Webster, K. A., Foster, S. L., Farrell, M. S., Ritchie, J. C., Porter, J. H., & Weinshenker, D. (2018). The DREADD agonist clozapine N-oxide (CNO) is reverse-metabolized to clozapine and produces clozapine-like interoceptive stimulus effects in rats and mice. *Scientific Reports*, *8*(1), 3840. <https://doi.org/10.1038/s41598-018-22116-z>
- Margolis, D. J., & Detwiler, P. B. (2007). Different Mechanisms Generate Maintained Activity in ON and OFF Retinal Ganglion Cells. *The Journal of Neuroscience*, *27*(22), 5994–6005. <https://doi.org/10.1523/JNEUROSCI.0130-07.2007>
- Martersteck, E. M., Hirokawa, K. E., Evarts, M., Bernard, A., Duan, X., Li, Y., Ng, L., Oh, S. W., Ouellette, B., Royall, J. J., Stoeklin, M., Wang, Q., Zeng, H., Sanes, J. R., & Harris, J. A. (2017). Diverse Central Projection Patterns of Retinal Ganglion Cells. *Cell Reports*, *18*(8), 2058–2072. <https://doi.org/10.1016/j.celrep.2017.01.075>
- Masland, R. H. (2001). The fundamental plan of the retina. *Nature Neuroscience*, *4*(9), 877–886. <https://doi.org/10.1038/nn0901-877>
- Matsumoto, A., Briggman, K. L., & Yonehara, K. (2019). Spatiotemporally Asymmetric Excitation Supports Mammalian Retinal Motion Sensitivity. *Current Biology*, *29*(19), 3277–3288.e5. <https://doi.org/10.1016/j.cub.2019.08.048>

- Morrie, R. D., & Feller, M. B. (2017). Motion Vision: Cortical Preferences Influenced by Retinal Direction Selectivity. *Current Biology*, 27(14), R710–R713.
<https://doi.org/10.1016/j.cub.2017.05.083>
- Moy, S. S., Nadler, J. J., Perez, A., Barbaro, R. P., Johns, J. M., Magnuson, T. R., Piven, J., & Crawley, J. N. (2004). Sociability and preference for social novelty in five inbred strains: An approach to assess autistic-like behavior in mice. *Genes, Brain and Behavior*, 3(5), 287–302. <https://doi.org/10.1111/j.1601-1848.2004.00076.x>
- Nikonov, S. S., Kholodenko, R., Lem, J., & Pugh, E. N. (2006). Physiological Features of the S- and M-cone Photoreceptors of Wild-type Mice from Single-cell Recordings. *Journal of General Physiology*, 127(4), 359–374.
<https://doi.org/10.1085/jgp.200609490>
- Pang, J.-J., Gao, F., & Wu, S. M. (2003). Light-Evoked Excitatory and Inhibitory Synaptic Inputs to ON and OFF α Ganglion Cells in the Mouse Retina. *The Journal of Neuroscience*, 23(14), 6063–6073. <https://doi.org/10.1523/JNEUROSCI.23-14-06063.2003>
- Pei, Z., Chen, Q., Koren, D., Giammarinaro, B., Ledesma, H. A., & Wei, W. (2015). Conditional Knock-Out of Vesicular GABA Transporter Gene from Starburst Amacrine Cells Reveals the Contributions of Multiple Synaptic Mechanisms Underlying Direction Selectivity in the Retina. *Journal of Neuroscience*, 35(38), 13219–13232. <https://doi.org/10.1523/JNEUROSCI.0933-15.2015>

- Poleg-Polsky, A., Ding, H., & Diamond, J. S. (2018). Functional Compartmentalization within Starburst Amacrine Cell Dendrites in the Retina. *Cell Reports*, 22(11), 2898–2908. <https://doi.org/10.1016/j.celrep.2018.02.064>
- Rasmussen, R. N., Matsumoto, A., Arvin, S., & Yonehara, K. (2021). Binocular integration of retinal motion information underlies optic flow processing by the cortex. *Current Biology*, 31(6), 1165–1174.e6. <https://doi.org/10.1016/j.cub.2020.12.034>
- Reese, B. E., & Galli-Resta, L. (2002). The role of tangential dispersion in retinal mosaic formation. *Progress in Retinal and Eye Research*, 21(2), 153–168. [https://doi.org/10.1016/S1350-9462\(01\)00024-6](https://doi.org/10.1016/S1350-9462(01)00024-6)
- Reinhard, K., Li, C., Do, Q., Burke, E. G., Heynderickx, S., & Farrow, K. (2019). A projection specific logic to sampling visual inputs in mouse superior colliculus. *eLife*, 8, e50697. <https://doi.org/10.7554/eLife.50697>
- Rheume, B. A., Jereen, A., Bolisetty, M., Sajid, M. S., Yang, Y., Renna, K., Sun, L., Robson, P., & Trakhtenberg, E. F. (2018). Single cell transcriptome profiling of retinal ganglion cells identifies cellular subtypes. *Nature Communications*, 9(1), 2759. <https://doi.org/10.1038/s41467-018-05134-3>
- Rodieck, R. W. (1998). *The First Steps in Seeing* (Illustrated edition). Sinauer Associates is an imprint of Oxford University Press.
- Sanes, J. R., & Masland, R. H. (2015). The Types of Retinal Ganglion Cells: Current Status and Implications for Neuronal Classification. *Annual Review of Neuroscience*, 38(1), 221–246. <https://doi.org/10.1146/annurev-neuro-071714-034120>

- Seabrook, T. A., Burbridge, T. J., Crair, M. C., & Huberman, A. D. (2017). Architecture, Function, and Assembly of the Mouse Visual System. *Annual Review of Neuroscience*, 40(1), 499–538. <https://doi.org/10.1146/annurev-neuro-071714-033842>
- Shen, Y., Heimel, J. A., Kamermans, M., Peachey, N. S., Gregg, R. G., & Nawy, S. (2009). A Transient Receptor Potential-Like Channel Mediates Synaptic Transmission in Rod Bipolar Cells. *Journal of Neuroscience*, 29(19), 6088–6093. <https://doi.org/10.1523/JNEUROSCI.0132-09.2009>
- Shi, Q., Gupta, P., Boukhvalova, A. K., Singer, J. H., & Butts, D. A. (2019). Functional characterization of retinal ganglion cells using tailored nonlinear modeling. *Scientific Reports*, 9(1), 8713. <https://doi.org/10.1038/s41598-019-45048-8>
- Simpson, J. I. (n.d.). *The Accessory Optic System*. 29.
- Soto, F., Hsiang, J.-C., Rajagopal, R., Piggott, K., Harocopos, G. J., Couch, S. M., Custer, P., Morgan, J. L., & Kerschensteiner, D. (2020). Efficient Coding by Midget and Parasol Ganglion Cells in the Human Retina. *Neuron*, 107(4), 656–666.e5. <https://doi.org/10.1016/j.neuron.2020.05.030>
- Tran, N. M., Shekhar, K., Whitney, I. E., Jacobi, A., Benhar, I., Hong, G., Yan, W., Adiconis, X., Arnold, M. E., Lee, J. M., Levin, J. Z., Lin, D., Wang, C., Lieber, C. M., Regev, A., He, Z., & Sanes, J. R. (2019). Single-Cell Profiles of Retinal Ganglion Cells Differing in Resilience to Injury Reveal Neuroprotective Genes. *Neuron*, 104(6), 1039–1055.e12. <https://doi.org/10.1016/j.neuron.2019.11.006>

- Twig, G., Levy, H., Weiner, E., & Perlman, I. (2003). Light adaptation and color opponency of horizontal cells in the turtle retina. *Visual Neuroscience*, 20(4), 437–452. <https://doi.org/10.1017/S0952523803204090>
- van Beest, E. H., Mukherjee, S., Kirchberger, L., Schnabel, U. H., van der Togt, C., Teeuwen, R. R. M., Barsegyan, A., Meyer, A. F., Poort, J., Roelfsema, P. R., & Self, M. W. (2021). Mouse visual cortex contains a region of enhanced spatial resolution. *Nature Communications*, 12(1), 4029. <https://doi.org/10.1038/s41467-021-24311-5>
- Varadarajan, S. G., & Huberman, A. D. (2018). Assembly and repair of eye-to-brain connections. *Current Opinion in Neurobiology*, 53, 198–209. <https://doi.org/10.1016/j.conb.2018.10.001>
- Wang, F., Li, E., De, L., Wu, Q., & Zhang, Y. (2021). OFF-transient alpha RGCs mediate looming triggered innate defensive response. *Current Biology*, 31(11), 2263–2273.e3. <https://doi.org/10.1016/j.cub.2021.03.025>
- Wassle, H., Puller, C., Muller, F., & Haverkamp, S. (2009). Cone Contacts, Mosaics, and Territories of Bipolar Cells in the Mouse Retina. *Journal of Neuroscience*, 29(1), 106–117. <https://doi.org/10.1523/JNEUROSCI.4442-08.2009>
- Wei, W. (2018). Neural Mechanisms of Motion Processing in the Mammalian Retina. *Annual Review of Vision Science*, 4(1), 165–192. <https://doi.org/10.1146/annurev-vision-091517-034048>
- Wiltchko, A. B., Johnson, M. J., Iurilli, G., Peterson, R. E., Katon, J. M., Pashkovski, S. L., Abaira, V. E., Adams, R. P., & Datta, S. R. (2015). Mapping Sub-Second Structure

in Mouse Behavior. *Neuron*, 88(6), 1121–1135.

<https://doi.org/10.1016/j.neuron.2015.11.031>

Yilmaz, M., & Meister, M. (2013). Rapid innate defensive responses of mice to looming visual stimuli. *Current Biology: CB*, 23(20), 2011–2015.

<https://doi.org/10.1016/j.cub.2013.08.015>

Yonehara, K., Ishikane, H., Sakuta, H., Shintani, T., Nakamura-Yonehara, K., Kamiji, N. L., Usui, S., & Noda, M. (2009). Identification of Retinal Ganglion Cells and Their Projections Involved in Central Transmission of Information about Upward and Downward Image Motion. *PLoS ONE*, 4(1), e4320.

<https://doi.org/10.1371/journal.pone.0004320>

Yoshida, K., Watanabe, D., Ishikane, H., Tachibana, M., Pastan, I., & Nakanishi, S. (2001). A Key Role of Starburst Amacrine Cells in Originating Retinal Directional Selectivity and Optokinetic Eye Movement. *Neuron*, 30(3), 771–780.

[https://doi.org/10.1016/S0896-6273\(01\)00316-6](https://doi.org/10.1016/S0896-6273(01)00316-6)

Yoshida, M., & Hasselmo, M. (2009). Persistent Firing Supported by an Intrinsic Cellular Mechanism in a Component of the Head Direction System. *The Journal of Neuroscience: The Official Journal of the Society for Neuroscience*, 29, 4945–4952.

<https://doi.org/10.1523/JNEUROSCI.5154-08.2009>